

# Heavy singly charged Higgs bosons and inverse seesaw neutrinos as origins of large $(g - 2)_{e,\mu}$ in two higgs doublet models

L. T. Hue,<sup>1,\*</sup> A. E. Cárcamo Hernández,<sup>2,3,4,†</sup> H. N. Long,<sup>1,‡</sup> and T. T. Hong<sup>d5,¶</sup>

<sup>1</sup>*Institute of Physics, Vietnam Academy of Science and Technology,*

*10 Dao Tan, Ba Dinh, Hanoi 10000, Vietnam*

<sup>2</sup>*Universidad Técnica Federico Santa María, Casilla 110-V, Valparaíso, Chile*

<sup>3</sup>*Centro Científico-Tecnológico de Valparaíso, Casilla 110-V, Valparaíso, Chile*

<sup>4</sup>*Millennium Institute for Subatomic Physics at High-Energy Frontier (SAPHIR),*

*Fernández Concha 700, Santiago, Chile*

<sup>5</sup>*An Giang University, VNU - HCM, Ung Van Khiem Street,*

*Long Xuyen, An Giang 88000, Vietnam*

## Abstract

We show that simple extensions of two higgs doublet models consisting of new heavy neutrinos and a singly charged Higgs boson singlet can successfully explain the experimental data on muon and electron anomalous magnetic moments thanks to large chirally-enhanced one-loop level contributions. These contributions arise from the large couplings of inverse seesaw neutrinos with singly charged Higgs bosons and right-handed charged leptons. The regions of parameter space satisfying the experimental data on  $(g - 2)_{e,\mu}$  anomalies allow heavy singly charged Higgs boson masses above the TeV scale, provided that heavy neutrino masses are above few hundred GeV, the non-unitary part of the active neutrino mixing matrix must be large enough, two singly charged Higgs bosons are non degenerate, and the mixing between singly charged Higgs bosons must be non-zero.

---

<sup>d</sup> Corresponding author

<sup>\*</sup> lthue1981@gmail.com

<sup>†</sup> antonio.carcamo@usm.cl

<sup>‡</sup> hnlong@iop.vast.vn

<sup>¶</sup> tthong@agu.edu.vn

## I. INTRODUCTION

The latest experimental measurement for the anomalous magnetic moment (AMM) of the muon  $a_\mu \equiv (g - 2)_\mu/2$  has been reported from Fermilab [1] and is in agreement with the previous experimental result measured by Brookhaven National Laboratory (BNL) E82 [2]. A combination of these results in the new average value of  $a_\mu^{\text{exp}} = 116592061(41) \times 10^{-11}$ , which leads to the improved standard deviation of  $4.2 \sigma$  from the Standard Model (SM) prediction, namely

$$\Delta a_\mu^{\text{NP}} \equiv a_\mu^{\text{exp}} - a_\mu^{\text{SM}} = (2.51 \pm 0.59) \times 10^{-9}, \quad (1)$$

where  $a_\mu^{\text{SM}} = 116591810(43) \times 10^{-11}$  is the SM prediction [3] combined from various different contributions [4–24]. On the other hand, the recent experimental  $a_e$  data was reported from different groups [25–27], leading to the latest deviation between experiment and the SM prediction [19, 28–33] as follows:

$$\Delta a_e^{\text{NP}} \equiv a_e^{\text{exp}} - a_e^{\text{SM}} = (4.8 \pm 3.0) \times 10^{-13}. \quad (2)$$

Many Beyond Standard Model (BSM) theories have been constructed to explain the  $(g - 2)_{\mu,e}$  anomalies. Such theories rely on the inclusion of vector-like lepton multiplets [34–50], leptoquarks [51–53], both neutral and charged Higgs bosons as  $SU(2)_L$  singlets [54, 55]. Some two Higgs doublet models (THDM) can provide sizeable two-loop contributions to  $\Delta a_\mu$  arising from new  $SU(2)_L$  Higgs doublets [56–61], where some of them require rather light masses of new neutral and/or charged Higgs boson masses at few hundred GeV.

There are many types of different versions of THDM, such as for instance: type I, type II, type X and type Y, which are discussed in Ref. [62], where collider phenomenology will give rise to different physical results. They are distinguished among themselves by the ways in which the two different  $SU(2)_L$  Higgs doublets  $\Phi_{1,2}$  generate the masses of up and down quarks as well as of charged leptons. These models arise from suitable choices of  $Z_2$  charge assignments. The Yukawa couplings of Higgs bosons with heavy fermions will be constrained by the perturbative limits, for example  $0.4 \leq \tan \beta \leq 91$  corresponding to the definitions of Yukawa couplings of the top and bottom quarks  $|Y_t| = (\sqrt{2}/v)m_t \cot \beta < \sqrt{\pi}$  and  $|Y_b| = (\sqrt{2}/v)m_b \tan \beta < \sqrt{\pi}$ , where  $\tan \beta$  is the ratio between the two vacuum expectation values (vevs) of the two neutral Higgs components. Discussions on the original THDM have shown that a new  $SU(2)_L$  Higgs doublet can be used to accommodate the  $(g - 2)_{e,\mu}$  anomalies

in a rather narrow allowed region of parameter space at the price of imposing dangerous requirements that can be experimentally tested in the near future [57, 63]. The conclusion is also true for the Minimal supersymmetric model MSSM [64–66]. As usual solution, there is a variety of extensions of THDM that successfully explain and accommodate the  $(g-2)_{e,\mu}$  anomalies by adding new vector-like fermions as  $SU(2)_L$  multiplets [38–43] as well as  $SU(2)_L$  singlets of neutral and charged Higgs bosons [54, 56, 68–71]. Only few THDM models with scalar singlets and fermions can successfully explain the experimental data of both muon and electron anomalous magnetic moments [42, 67, 69]. Our work here will introduce a more general solution that a wide class of the THDM by adding heavy right handed (RH) neutrino singlets and one singly electrically charged Higgs bosons can give sizeable one-loop contributions enough to explain the experimental ranges of values of both muon and electron anomalous magnetic moments in a wide region of parameter space.

This paper is organized as follows. In Sec. II, the THDM extension with new RH neutrinos and singly charged Higgs boson ( $\text{THDM}N_R h^\pm$ ) will be introduced, where we pay attention to the leptons, gauge bosons, and Higgs sectors, giving all physical states as well the couplings that may give large one-loop contributions to AMM. In Sec. III, the simple inverse seesaw (ISS) and analytic formulas for one-loop contributions to AMM are constructed. Numerical discussion will be shown in details. Our main results will be collected in Sec. IV.

## II. REVIEW OF THE $\text{THDM}N_R h^\pm$

In this section we will focus on the analysis of the lepton sector of the  $\text{THDM}N_R h^\pm$ . For details of the quark sector of different types of the THDM, the reader is referred to Refs. [72, 73]. The leptonic, quark and scalar spectrum with their assignments under the  $SU(2)_L \times U(1)_Y$  gauge group are given by [72, 73]:

$$\begin{aligned}
L_a &= \begin{pmatrix} \nu_{aL} \\ e_{aL} \end{pmatrix} \sim (2, -1); \quad Q_{aL} = \begin{pmatrix} u_{aL} \\ d_{aL} \end{pmatrix} \sim \left(2, \frac{1}{3}\right), \\
e_{aR} &\sim (1, -2); \quad u_{aR} \sim \left(1, \frac{4}{3}\right); \quad d_{aR} \sim \left(1, -\frac{2}{3}\right); \quad N_{IR} \sim (1, 0), \quad a = 1, 2, 3, \quad I = 1, 2, \dots, 6; \\
\Phi_i &= \begin{pmatrix} \phi_i^+ \\ \phi_i^0 \end{pmatrix} \sim (2, 1), \quad \langle \Phi_i \rangle = \begin{pmatrix} 0 \\ \frac{v_i}{\sqrt{2}} \end{pmatrix} \sim (2, 1), \quad i = 1, 2; \\
h^\pm &\sim (1, \pm 2).
\end{aligned} \tag{3}$$

Note that we use the old convention for the defining the hypercharge via the original Gell-Mann-Nishima relation:

$$Q = T_3 + \frac{1}{2}Y \quad (4)$$

Here we add six new neutrino singlets to the leptonic spectrum of the model in order to implement the standard ISS mechanism. Furthermore, the model scalar sector is augmented by the inclusion of singly charged Higgs bosons, which allow to generate the new Yukawa interaction  $\overline{(N_{IR})^c} e_{aR} h^+$  thus resulting in sizeable one-loop contributions to AMM.

One of the most important parameters introduced in the THDM is

$$t_\beta \equiv \tan \beta = \frac{v_2}{v_1}, \quad s_\beta \equiv \sin \beta, \quad c_\beta \equiv \cos \beta. \quad (5)$$

We will also follow the notations  $s_x \equiv \sin x$ ,  $c_x \equiv \cos x$ , and  $t_x = s_x/c_x$  for any parameter  $x$ . Because the Yukawa couplings of up type quarks and  $\Phi_2$  are fixed, we always have a lower bound  $t_\beta \geq 0.4$ . In the THDM type I, all fermions couple with only  $\Phi_2$ , hence no upper bounds for  $t_\beta$  arise. In the THDM type II and Y, all down type quarks and charged leptons couple with  $\Phi_1$ , hence  $t_\beta \leq 91$ . In the type-X, the Yukawa coupling of tau with  $\Phi_1$  gives  $t_\beta \leq 348$ .

The THDM type-II and type-X where lepton doublets couple with only  $\Phi_1$  are called THDM type-A. The corresponding lepton Yukawa terms are:

$$\begin{aligned} -\mathcal{L}_\ell^Y = & Y_{ab}^e \overline{e_{aR}} \Phi_1^\dagger L_b + Y_{k,Ia}^N \overline{N_{IR}} (i\sigma_2 \Phi_k)^T L_a + \frac{1}{2} M_{N,IJ} \overline{N_{IR}} (N_{JR})^c \\ & + Y_{Ia}^h \overline{(N_{IR})^c} e_{aR} h^+ + \text{h.c.}, \end{aligned} \quad (6)$$

where  $a, b = 1, 2, 3$  are family indices;  $k = 1, 2$ ; and  $I = 1, 2, 3, \dots, 6$  are the number of new neutral lepton singlets. A rough condition for the perturbative limit of  $Y^h$  is  $|Y_{Ia}^h| < \sqrt{4\pi}$ , and should be smaller for trusty values [74]. The  $Z_2$  charges of  $N_{IR}$  and  $h$  are always chosen to guarantee the  $Z_2$  symmetry of Lagrangian (6). Using the  $Z_2$  charge assignments discussed in Ref. [62], two Higgs triplets  $\Phi_1$  have different  $Z_2$  charges, therefore  $N_{IR}$  coupling with only one of them.

In the THDM type-I and type-Y, where charged lepton couple with  $\Phi_2$ , the first term of Eq. (6) should replace  $\Phi_1$  with  $\Phi_2$ . We call them the THDM type-B and will discuss later that the qualitative results for AMM do not change. This model type including the model introduced in Ref. [42].

We also emphasize that the models under consideration including the Yukawa part discussed on Ref. [54] focusing on one particular case of  $\Phi_k = \Phi_2$ . As we will show that in our numerical analysis, the regions of the parameter space predicting  $\Delta a_{e,\mu}$  consistent with the experimental data, favor small values of  $t_\beta$ , including the range  $t_\beta \in [0.4, 10]$  which was not mentioned in Ref. [54].

Defining  $\nu'_L = (\nu_1, \nu_2, \nu_3)_L^T$  and  $N_R = (N_1, N_2, \dots, N_6)_R^T$ , we find the following leptonic mass terms:

$$-\mathcal{L}_{\text{lepton}}^{\text{mass}} = \frac{Y_{ab}^e v_1}{\sqrt{2}} \overline{e'_{aR}} e'_{bL} + \frac{1}{2} \left( \overline{(\nu'_L)^c} \ N_R \right) \mathcal{M}^\nu \begin{pmatrix} \nu'_L \\ (N_R)^c \end{pmatrix} + \text{h.c.}, \quad \mathcal{M}^\nu = \begin{pmatrix} 0_{3 \times 3} & M_D^T \\ M_D & M_N \end{pmatrix}, \quad (7)$$

where

$$(M_D)_{Ia} \equiv M_{D,Ia} = \sum_{k=1}^2 \frac{Y_{k,Ia}^N v_k}{\sqrt{2}} \quad (8)$$

are the components of a  $6 \times 3$  Dirac neutrino mass matrix and  $M_N$  is a  $6 \times 6$  symmetric Majorana mass matrix. Here we choose basis where the charged lepton mass matrix is diagonal, which implies  $Y_{ab}^e = \delta_{ab} \sqrt{2} m_{e_a} / v_1$ , i.e., the flavor and mass states of charged leptons are the same. The total unitary mixing matrix is defined as

$$U^{\nu T} \mathcal{M}^\nu U^\nu = \hat{\mathcal{M}}^\nu = \text{diag}(m_{n_1}, m_{n_1}, \dots, m_{n_{(K+3)}}) \equiv \text{diag}(\hat{m}_\nu, \hat{M}_N),$$

$$\begin{pmatrix} \nu'_L \\ (N_R)^c \end{pmatrix} = U^\nu n_L, \quad \begin{pmatrix} (\nu'_L)^c \\ N_R \end{pmatrix} = U^{\nu*} n_R = U^{\nu*} (n_L)^c, \quad (9)$$

where  $n_{L,R} = (n_1, n_2, \dots, n_9)_{L,R}$  are the Majorana neutrino mass eigenstates satisfying  $n_{iL,R} = (n_{iR,L})^c$ , and the four-component forms are  $n_i = (n_{iL}, n_{iR})^T$ .

Given that we are working in the basis where the charged lepton mass matrix is diagonal, the leptonic mixing entirely arises from the neutrino sector. This implies that, in order to successfully reproduce the neutrino oscillation experimental data, the neutrino mixing matrix is parameterised in the following form:

$$U^\nu = \begin{pmatrix} \left( I_3 - \frac{1}{2} R R^\dagger \right) U_{\text{PMNS}} & RV \\ -R^\dagger U_{\text{PMNS}} & \left( I_6 - \frac{1}{2} R^\dagger R \right) V \end{pmatrix} + \mathcal{O}(R^3), \quad (10)$$

where  $V$  is a  $6 \times 6$  unitary matrix;  $R$  is a  $3 \times 6$  matrix satisfying  $|R_{aI}| < 1$  for all  $a = 1, 2, 3$ , and  $I = 1, 2, \dots, 6$ . The  $3 \times 3$  unitary matrix  $U_{\text{PMNS}}$  is the Pontecorvo-Maki-Nakagawa-Sakata (PMNS) matrix [75].

The successful implementation of the ISS mechanism requires to construct the Dirac and Majorana mass matrices in terms of  $3 \times 3$  submatrices as follows [76, 77]

$$M_D^T = (m_D^T, 0_{3 \times 3}), \quad M_N = \begin{pmatrix} 0_{3 \times 3} & M_R \\ M_R^T & \mu_X \end{pmatrix}, \quad (11)$$

where  $0_{3 \times 3}$  is the  $3 \times 3$  null matrix. Using a new notation  $M = M_R \mu_X^{-1} M_R^T$ . we have the following ISS relations:

$$\begin{aligned} R &= M_D^\dagger M_N^{*-1} = \begin{pmatrix} -m_D^\dagger M^{*-1}, & m_D^\dagger (M_R^\dagger)^{-1} \end{pmatrix}, \\ U_{\text{PMNS}}^* \hat{m}_\nu U_{\text{PMNS}}^\dagger &= m_\nu = -M_D^T M_N^{-1} M_D = m_D^T (M_R^T)^{-1} \mu_X M_R^{-1} m_D, \\ V^* \hat{M}_N V^\dagger &\simeq M_N + \frac{1}{2} R^T R^* M_N + \frac{1}{2} M_N R^\dagger R. \end{aligned} \quad (12)$$

Because  $m_D$  is parameterized in terms of many free parameters, hence it is enough to choose  $\mu_X = \mu_0 I_3$  with  $\mu_0 > 0$ ,  $M_R = \hat{M}_R = M_0 I_3$ . We choose a simple form  $m_D = \frac{M_0}{\sqrt{\mu_0}} \sqrt{\hat{m}_\nu} U_{\text{PMNS}}^\dagger$  [76–78]. The ISS condition  $|\hat{m}_\nu| \ll |\mu_X| \ll |m_D| \ll M_0$  gives  $\frac{\sqrt{\mu_0} \hat{m}_\nu}{M_0} \simeq 0$  and

$$\hat{M}_N = \begin{pmatrix} \hat{M}_R & 0_{3 \times 3} \\ 0_{3 \times 3} & \hat{M}_R \end{pmatrix} \simeq M_0 I_6, \quad V \simeq \frac{1}{\sqrt{2}} \begin{pmatrix} -iI_3 & I_3 \\ iI_3 & I_3 \end{pmatrix}, \quad (13)$$

meaning that all of six heavy neutrinos have approximately the same mass  $m_{n_i} \simeq M_0$  for all  $i > 3$ . Hence, the above simple forms of  $M_R$ , and  $\mu_X$  will result in degenerate heavy neutrino masses, leading to small rates of lepton flavor violating decays of charged leptons (cLFV) that satisfy the current experimental constraints [79, 80]. Relations in (12) reduce to the following simple forms:

$$m_D = M_0 \hat{x}_\nu^{1/2} U_{\text{PMNS}}^\dagger, \quad R = \left( -U_{\text{PMNS}} \frac{\sqrt{\mu_0 \hat{m}_\nu}}{M_0}, \ U_{\text{PMNS}} \hat{x}_\nu^{1/2} \right) \simeq (0_{3 \times 3}, \ U_{\text{PMNS}} \hat{x}_\nu^{1/2}), \quad (14)$$

where

$$\hat{x}_\nu \equiv \frac{\hat{m}_\nu}{\mu_0} \equiv \text{diag}(\hat{x}_{\nu 1}, \hat{x}_{\nu 2}, \hat{x}_{\nu 3}), \quad \hat{x}_{\nu a} \equiv \frac{m_{n_a}}{\mu_0}, \quad a = 1, 2, 3 \quad (15)$$

satisfying  $\max[|\hat{x}_{\nu a}|] \ll 1$  for all  $a = 1, 2, 3$ .

In our numerical analysis, we will use the best-fit values of the neutrino oscillation data [75] corresponding to the normal order (NO) scheme with  $m_{n_1} < m_{n_2} < m_{n_3}$ , namely

$$\begin{aligned} s_{12}^2 &= 0.32, \ s_{23}^2 = 0.547, \ s_{13}^2 = 0.0216, \ \delta = 218 \text{ [Deg]}, \\ \Delta m_{21}^2 &= 7.55 \times 10^{-5} \text{ [eV}^2], \ \Delta m_{32}^2 = 2.424 \times 10^{-3} \text{ [eV}^2]. \end{aligned} \quad (16)$$

In order to simplify our numerical analysis, we assume  $0 \simeq m_{n_1} \ll m_{n_2} < m_{n_3}$ . Furthermore, we have the relations:

$$\begin{aligned}\hat{x}_\nu &= \mu_0^{-1} \text{diag} \left( m_{n_1}, \sqrt{m_{n_1}^2 + \Delta m_{21}^2}, \sqrt{m_{n_1}^2 + \Delta m_{21}^2 + \Delta m_{32}^2} \right), \\ U_{\text{PMNS}} &= \begin{pmatrix} c_{12}c_{13} & c_{13}s_{12} & s_{13}e^{-i\delta} \\ -c_{23}s_{12} - c_{12}s_{13}s_{23}e^{i\delta} & c_{23}^2 - s_{12}s_{13}s_{23}e^{i\delta} & c_{13}s_{23} \\ s_{12}s_{23} - c_{12}c_{23}s_{13}e^{i\delta} & -c_{23}s_{12}e^{i\delta}s_{13} - c_{23}s_{23} & c_{13}c_{23} \end{pmatrix} \\ &\simeq \begin{pmatrix} 0.816 & 0.560 & 0.147e^{-i\delta} \\ -0.381 - 0.09e^{i\delta} & 0.453 - 0.062e^{i\delta} & 0.732 \\ 0.418 - 0.082e^{i\delta} & -0.498 - 0.056e^{i\delta} & 0.666 \end{pmatrix}. \end{aligned} \quad (17)$$

These numerical values of neutrino masses satisfy the cosmological constraint arising from the Plank 2018 [81]:  $\sum_{i=a}^3 m_{n_a} \leq 0.12$  eV.

The other well-known numerical parameters are given in Ref. [75], namely

$$\begin{aligned}g &= 0.652, \quad \alpha_e = \frac{1}{137} = \frac{e^2}{4\pi}, \quad s_W^2 = 0.231, \\ m_e &= 5 \times 10^{-4} \text{ GeV}, \quad m_\mu = 0.105 \text{ GeV}, \quad m_W = 80.385 \text{ GeV}. \end{aligned} \quad (18)$$

Also the inverted order (IO) scheme with  $m_{n_3} < m_{n_1} < m_{n_2}$  can be considered in the similar way, but the qualitative results are the same with those from NO scheme, so we will not present here.

The non-unitary of the active neutrino mixing matrix  $(I_3 - \frac{1}{2}RR^\dagger) U_{\text{PMNS}}$  is constrained by other phenomenological aspects such as, for instance, electroweak precision tests, cLFV decays [82–84], thus leading to the following constraints

$$\eta \equiv \frac{1}{2} |RR^\dagger| < \eta_0 = \begin{pmatrix} 2 \times 10^{-3} & 3.5 \times 10^{-5} & 8. \times 10^{-3} \\ 3.5 \times 10^{-5} & 8 \times 10^{-4} & 5.1 \times 10^{-3} \\ 8 \times 10^{-3} & 5.1 \times 10^{-3} & 2.7 \times 10^{-3} \end{pmatrix}. \quad (19)$$

This constraint is consistent with the data popularly used in recent works discussion on the ISS framework [54, 85]. The constraint on  $\eta$  may be more strict, depending on particular models. For example in the type general III and inverse seesaw models, one has the constraint  $|\eta_{aa}| \leq \mathcal{O}(10^{-4})$  [36, 86]. In our numerical analysis, we will choose the values satisfying  $|\eta_{33}| \leq 10^{-3}$ .

In the next section, we will discuss the model scalar potential as well as the one-loop contributions to  $\Delta a_{\mu,e}$ .

### III. HIGGS BOSONS AND ONE-LOOP CONTRIBUTIONS TO $\Delta a_{e_a}$

In the Higgs potential, the two Higgs doublets  $\Phi_i$  are changed into a new basis as follows:

$$\begin{pmatrix} H_1 \\ H_2 \end{pmatrix} = \begin{pmatrix} c_\beta & s_\beta \\ -s_\beta & c_\beta \end{pmatrix} \begin{pmatrix} \Phi_1 \\ \Phi_2 \end{pmatrix}. \quad (20)$$

where  $t_\beta \equiv \tan \beta = \frac{v_2}{v_1}$ ,  $s_x \equiv \sin x$  and  $c_x \equiv \cos x$ . These two Higgs doublets can be expanded around the minimum as shown below:

$$H_1 = \begin{pmatrix} G^+ \\ \frac{v + \varphi_1^0 + iG^0}{\sqrt{2}} \end{pmatrix}, \quad H_2 = \begin{pmatrix} H^+ \\ \frac{\varphi_2^0 + iA}{\sqrt{2}} \end{pmatrix}. \quad (21)$$

The Higgs potential after the transformation (20) takes the form [72]

$$\begin{aligned} V = & \mu_1^2 H_1^\dagger H_1 + \mu_2^2 H_2^\dagger H_2 - \left( \mu_3^2 H_2^\dagger H_1 + \text{H.c.} \right) \\ & + \frac{1}{2} \lambda_1 \left( H_1^\dagger H_1 \right)^2 + \frac{1}{2} \lambda_2 \left( H_2^\dagger H_2 \right)^2 + \lambda_3 \left( H_1^\dagger H_1 \right) \left( H_2^\dagger H_2 \right) + \lambda_4 \left( H_1^\dagger H_2 \right) \left( H_2^\dagger H_1 \right) \\ & + \left[ \frac{1}{2} \lambda_5 \left( \left( H_1^\dagger H_2 \right)^2 + \left[ \lambda_6 \left( H_1^\dagger H_1 \right) + \lambda_7 \left( H_2^\dagger H_2 \right) \right] \left( H_1^\dagger H_2 \right) + \text{H.c.} \right] \right. \\ & \left. + \lambda_h \left| h^+ \right|^4 + \left| h^+ \right|^2 \left[ \mu_h^2 + \lambda_8 H_1^\dagger H_1 + \lambda_9 H_2^\dagger H_2 + \lambda_{10} \left( H_1^\dagger H_2 + \text{H.c.} \right) \right] \right. \\ & \left. + \left( \mu \epsilon_{\alpha\beta} H_1^\alpha H_2^\beta h^- + \text{H.c.} \right) \right]. \end{aligned} \quad (22)$$

The physical charged scalar states and their masses are given by:

$$\begin{pmatrix} h_1^\pm \\ h_2^\pm \end{pmatrix} = \begin{pmatrix} s_\varphi & c_\varphi \\ c_\varphi & -s_\varphi \end{pmatrix} \begin{pmatrix} h^\pm \\ H^\pm \end{pmatrix}, \quad s_{2\varphi} = \frac{\sqrt{2}v\mu}{m_{h_2^+}^2 - m_{h_1^+}^2},$$

$$m_{h_1^+, h_2^+}^2 \equiv \frac{1}{2} \left[ M_{H^+}^2 + M_{33}^2 \mp \sqrt{\left( M_{H^+}^2 - M_{33}^2 \right)^2 + 2v^2\mu^2} \right], \quad (23)$$

where  $M_{H^+}^2 = \mu_2^2 + \frac{1}{2}v^2\lambda_3$ ,  $M_{33}^2 = \mu_h^2 + v^2\lambda_8$ .

In our numerical calculation, we will use  $m_{h_k^+}^2$  and the mixing angle  $\varphi$  as free parameters. Three Higgs mass parameters  $\mu_2^2$ ,  $\mu_h^2$ , and  $\mu$  are functions of the remaining parameters. Thus, no perturbative limits on the Higgs selfcouplings are necessary to constrain the dependent functions chosen here.

From the above information we obtain all vertices providing one-loop contributions to the  $e_b \rightarrow e_a \gamma$  decay rates as well as to  $\Delta a_{e_a}$ . They are collected from the lepton Yukawa

terms given in Eq. (6), namely

$$\mathcal{L}_{\text{lepton}}^{\text{yuk}} = -\frac{gm_{e_a}(-t_\beta)}{\sqrt{2}m_W} \overline{L_a} H_2 e_{aR} - Y_{0,Ia}^N \overline{N_{IR}} (i\sigma_2 H_2)^T L_a - Y_{Ia}^h \overline{(N_{IR})^c} e_{aR} h^+ + \text{h.c.}, \quad (24)$$

where we denote  $Y_0^N \equiv (0_{3 \times 3}, Y_0^N)^T = -s_\beta Y_1^N + c_\beta Y_2^N$  for the ISS mechanism discussed in this work. It is interesting to link this matrix with  $M_D$  given in Eq. (8), where depending on the  $Z_2$  charges of  $N_{IR}$  there are two cases where non-zero couplings with only  $\Phi_1$  or  $\Phi_2$  correspond to  $Y_2^N = 0$  or  $Y_1^N = 0$ , respectively. Namely

$$M_D^T = \left( 0_{3 \times 3}, \frac{vf_H^{-1}}{\sqrt{2}} Y_0^N \right)^T, \quad f_H = \begin{cases} t_\beta^{-1}, & Y_1^N = 0_{6 \times 3}, Y_2^N \neq 0; \\ -t_\beta, & Y_2^N = 0_{6 \times 3}, Y_1^N \neq 0 \end{cases}. \quad (25)$$

With this new notation, the Yukawa Lagrangian for the THDM type-A is

$$\begin{aligned} \mathcal{L}_{\text{lepton}}^{\text{yuk}} = & \frac{gm_{e_a}t_\beta}{\sqrt{2}m_W} U_{ai}^{\nu*} \overline{n_{iL}} e_{aR} (c_\varphi h_1^+ - s_\varphi h_2^+) + \frac{gf_H}{\sqrt{2}m_W} U_{(I+3)i}^\nu M_{D,ia} \overline{n_{iR}} e_{aL} (c_\varphi h_1^+ - s_\varphi h_2^+) \\ & - Y_{Ib}^h U_{(I+3)i}^{\nu*} \overline{n_{iL}} e_{aR} (s_\varphi h_1^+ + c_\varphi h_2^+) + \text{h.c.} \end{aligned} \quad (26)$$

Then, all relevant couplings are given in the following lepton Yukawa interaction Lagrangian

$$\mathcal{L} = \sum_{a=1}^3 \sum_{i=1}^9 \left[ \frac{g}{\sqrt{2}m_W} \sum_{k=1}^2 \overline{n_i} \left( \lambda_{ia}^{L,k} P_L + \lambda_{ia}^{R,k} P_R \right) e_a h_k^+ + \frac{g}{\sqrt{2}} U_{ai}^{\nu*} \overline{n_i} \gamma^\mu P_L e_a W_\mu^+ \right] + \text{h.c.}, \quad (27)$$

where

$$\begin{aligned} \lambda_{ia}^{L,1} &= \sum_{I=1}^6 f_H M_{D,Ia} c_\varphi U_{(I+3)i}^\nu \simeq f_H c_\varphi \times \begin{cases} 0, & i \leq 3 \\ (M_D^T V)_{a(i-3)}, & i > 3 \end{cases}, \\ \lambda_{ia}^{L,2} &\simeq -\lambda_{ia}^{L,1} t_\varphi = \lambda_{ia}^{L,1} [c_\varphi \rightarrow -s_\varphi], \\ \lambda_{ia}^{R,1} &= m_{e_a} t_\beta c_\varphi U_{ai}^{\nu*} - \sum_{I=1}^6 \frac{v}{\sqrt{2}} s_\varphi Y_{Ia}^h U_{(I+3)i}^{\nu*} \\ &\simeq \begin{cases} m_{e_a} t_\beta c_\varphi [U_{\text{PMNS}}^* (I_3 - \frac{1}{2} \hat{x}_\nu)]_{ai} + \frac{v s_\varphi}{\sqrt{2}} (Y^{hT} R^T U_{\text{PMNS}}^*)_{ai}, & i \leq 3 \\ m_{e_a} t_\beta c_\varphi (R V)_{a(i-3)}^* - \frac{v s_\varphi}{\sqrt{2}} [Y^{hT} (I_6 - \frac{1}{2} R^T R^*) V^*]_{a(i-3)} & i > 3 \end{cases}, \\ \lambda_{ia}^{R,2} &= -m_{e_a} t_\beta s_\varphi U_{ai}^{\nu*} - \sum_{I=1}^6 \frac{v}{\sqrt{2}} c_\varphi Y_{Ia}^h U_{(I+3)i}^{\nu*} \\ &\simeq \begin{cases} -m_{e_a} t_\beta s_\varphi [U_{\text{PMNS}}^* (I_3 - \frac{1}{2} \hat{x}_\nu)]_{ai} + \frac{v c_\varphi}{\sqrt{2}} (Y^{hT} R^T U_{\text{PMNS}}^*)_{ai}, & i \leq 3 \\ -m_{e_a} t_\beta s_\varphi (R V)_{a(i-3)}^* - \frac{v c_\varphi}{\sqrt{2}} [Y^{hT} (I_6 - \frac{1}{2} R^T R^*) V^*]_{a(i-3)} & i > 3 \end{cases} \end{aligned}$$

$$= \lambda_{ia}^{R,1} [s_\varphi \rightarrow c_\varphi, c_\varphi \rightarrow -s_\varphi]. \quad (28)$$

We do not list here the couplings of neutral gauge and Higgs bosons because they give suppressed contributions to  $a_{e_a}^{\text{NP}}$ . In particular, the relevant couplings are only the ones with usual charged leptons  $s^0 \bar{e}_a e_a$  and  $Z_\mu \bar{e}_a \gamma^\mu e_a$ . The one-loop level contribution arising from the  $Z$  gauge boson exchange is the same as the predicted by the SM. The contributions arising from new neutral Higgs bosons are not larger than the one coming from the SM-like Higgs boson since they are suppressed by a factor of the order of  $\mathcal{O}(10^{-14})$ , because we assume here their masses are at the TeV scale.

We will use the approximation that  $m_{n_i}^2/m_W^2 = 0$  with  $i \leq 3$  and  $m_{n_i}^2/m_W^2 = M_0^2/m_W^2 = x_W$  with  $i > 3$ . Then, the contribution to  $a_{e_a}$  arising from the  $W$  exchange has the form:

$$a_{e_a}(W) = -\frac{g^2 m_{e_a}^2}{8\pi^2 m_W^2} \left[ -\frac{5}{12} + (R^* R^T)_{aa} \times \left( \tilde{f}_V(x_W) + \frac{5}{12} \right) \right], \quad (29)$$

where

$$\begin{aligned} \tilde{f}_V(x) &= \frac{-4x^4 + 49x^3 - 78x^2 + 43x - 10 - 18x^3 \ln x}{24(x-1)^4}, \\ \tilde{f}_V(0) &= -\frac{5}{12} \leq \tilde{f}_V(x) \leq \tilde{f}_V(\infty) = -\frac{1}{6}. \end{aligned} \quad (30)$$

Because  $|\tilde{f}_V(x_W) + \frac{5}{12}| \leq \frac{5}{12}$  and  $(R^* R^T)_{aa} \leq \mathcal{O}(10^{-3}) \ll 1$ , Eq. (29) equals to the one-loop level contribution predicted by the SM, see example in Ref. [87]:

$$a_\mu^{(1)\text{SM}}(W) = \frac{g^2 m_\mu^2}{8\pi^2 m_W^2} \times \frac{5}{12} \simeq 383 \times 10^{-11}, \quad \frac{g^2 m_\mu^2}{8\pi^2 m_W^2} \simeq 9.19 \times 10^{-9}. \quad (31)$$

The one-loop level contribution to  $\Delta a_{e_a}$  arising from the exchange of the electrically charged scalar singlet  $h_k^\pm$  is given by [35]:

$$a_{e_a}(h_k^\pm) = -\frac{g^2 m_{e_a}}{8\pi^2 m_W^2} \sum_{i=1}^9 \frac{\lambda_{ia}^{L,k*} \lambda_{ia}^{R,k} m_{n_i} f_\Phi(x_{i,k}) + m_{e_a} \left( \lambda_{ia}^{L,k*} \lambda_{ia}^{L,k} + \lambda_{ia}^{R,k*} \lambda_{ia}^{R,k} \right) \tilde{f}_\Phi(x_{i,k})}{m_{h_k^\pm}^2}, \quad (32)$$

where  $x_{i,k} \equiv m_{n_i}^2/m_{h_k^\pm}^2$ ,  $f_a = \frac{g^2 m_{e_a}}{8\pi^2 m_W^2} > 0$ , and the loop functions appearing in Eq. (32) have the forms:

$$\begin{aligned} f_\Phi(x) &= \frac{x^2 - 1 - 2x \ln x}{4(x-1)^3}, \\ \tilde{f}_\Phi(x) &= \frac{2x^3 + 3x^2 - 6x + 1 - 6x^2 \ln x}{24(x-1)^4}, \end{aligned}$$

$$\begin{aligned} f_\Phi(\infty) &= 0 \leq f_\Phi(x) \leq f_\Phi(0) = \frac{1}{4}, \\ \tilde{f}_\Phi(\infty) &= 0 \leq \tilde{f}_\Phi(x) \leq \tilde{f}_\Phi(0) = \frac{1}{24}. \end{aligned} \quad (33)$$

And the deviation from the SM is defined as follows:

$$\Delta a_{e_a} = \sum_{k=1}^2 a_{e_a}(h_k^\pm) + \Delta a_{e_a}(W), \quad \Delta a_{e_a}(W) \equiv a_{e_a}(W) - a_{e_a}^{(1)\text{SM}}(W), \quad (34)$$

where  $a_\mu^{(1)\text{SM}}(W) \simeq 3.83 \times 10^{-9}$  [87].

Using the approximations  $m_{n_i}^2/m_{h_k^\pm}^2 \simeq 0$  for  $i \leq 3$  and  $m_{n_i}^2/m_{h_k^\pm}^2 \simeq M_0^2/m_{h_k^\pm}^2 = x_k$ , we have  $f_\Phi(x_{i,k}) \simeq f_\Phi(0)$  for  $i \leq 3$  and  $f_\Phi(x_{i,k}) \simeq f_\Phi(x_k)$  for  $i > 3$ . Following Eqs. (13) and (14), we obtain that the one loop level contribution to  $a_{e_a}$  due to the exchange of  $h_1^\pm$  is given by

$$\begin{aligned} a_{e_a}(h_1^\pm) &= -9.19 \times 10^{-9} \times \frac{m_{e_a}^2}{m_\mu^2} \\ &\times \text{Re} \left\{ \sum_{c=1}^3 f_H \left[ c_\varphi^2 t_\beta |U_{\text{PMNS},ac}|^2 \frac{m_{n_c}}{\mu_0} - \frac{v c_\varphi s_\varphi}{\sqrt{2} m_{e_a}} U_{\text{PMNS},ac} \left( \frac{m_{n_c}}{\mu_0} \right)^{1/2} Y_{(c+3)a}^h \right] x_1 f_\Phi(x_1) \right. \\ &+ \sum_{c=1}^3 \left[ |U_{\text{PMNS},ac}|^2 \left( f_H^2 c_\varphi^2 \frac{m_{n_c}}{\mu_0} \right) \right] x_1 \tilde{f}_\Phi(x_1) \\ &+ \frac{m_{e_a}^2 t_\beta^2 c_\varphi^2}{m_{H_1^\pm}^2} \left[ \frac{1}{24} - \sum_{c=1}^3 \left[ |U_{\text{PMNS},ac}|^2 \frac{m_{n_c}}{\mu_0} \right] \left( \frac{1}{24} - \tilde{f}_\Phi(x_1) \right) \right] \\ &+ \frac{v^2 s_\varphi^2}{2 m_{H_1^\pm}^2} \left[ \sum_{c=1}^3 \left[ |Y_{(c+3)a}^h|^2 \frac{m_{n_c}}{\mu_0} \right] \left( \frac{1}{24} - \tilde{f}_\Phi(x_1) \right) + (Y^{h\dagger} Y^h)_{aa} \tilde{f}_\Phi(x_1) \right] \\ &\left. - \frac{v m_{e_a} t_\beta s_{2\varphi}}{\sqrt{2} m_{H_1^\pm}^2} \left( \frac{1}{24} - \tilde{f}_\Phi(x_1) \right) \sum_{c=1}^3 \left[ U_{\text{PMNS},ac} Y_{(c+3)a}^h \left( \frac{m_{n_c}}{\mu_0} \right)^{1/2} \right] \right\}, \end{aligned} \quad (35)$$

$$a_\mu^{\text{ISS}}(h_2^\pm) = a_\mu(h_1^\pm) [x_1 \rightarrow x_2, s_\varphi \rightarrow c_\varphi, c_\varphi \rightarrow -s_\varphi]. \quad (36)$$

In the real part of Eq. (35), the first line corresponds to the chirally-enhanced part proportional to  $\lambda^{L,1*} \lambda^{R,1*}$  whereas the second and remaining lines are the parts proportional to  $\lambda^{L,1*} \lambda^{L,1*}$  and  $\lambda^{R,1*} \lambda^{R,1*}$ , respectively.

Now we compare our results given in Eq. (35) with the one-loop contribution due to the exchange of singly electrically charged Higgs bosons in the original versions [62] without  $N_{IR}$  and the singlet  $h^\pm$ . Now we assume  $h_1^\pm \equiv H^\pm$  in Eq. (23), corresponding to  $c_\varphi = 1, s_\varphi = 0$ . The absence of  $N_{IR}$  can be conveniently derived from  $f_H = 0$  and  $f(x_1) = 0$ , thus implying

that the only one-loop contribution from  $h_1^\pm$  only consists of the first term in the third line of the real part given in Eq. (35), which is proportional to  $-9.19 \times 10^{-9} \times m_{e_a}^4 t_\beta^2 c_\varphi^2 / (24 m_\mu^2 m_{H_1^\pm}^2)$ , which yields a small and negative contribution to  $\Delta a_\mu^{\text{NP}}$  [63]. The dominant contributions to AMM arise from two-loop Barr-Zee type diagrams. The similar conclusion for the THDM type-B where  $t_\beta^2 \rightarrow t_\beta^{-2}$ , hence has suppressed two-loop contributions to AMM for  $t_\beta \geq 0.4$ .

If the mixing between two singly charged Higgs bosons vanishes, namely  $s_\alpha c_\alpha = 0$ , then all of the remaining terms in both Eqs. (35) and (36) are negative, thus not allowing to accommodate the experimental data on muon and electron anomalous magnetic moments.

Using the constraint (19) for  $RR^\dagger = U_{\text{PMNS}} \hat{x}_\nu U_{\text{PMNS}}^\dagger$  we have  $\hat{x}_\nu < \mathcal{O}(10^{-3})$ . Therefore, we will choose a safe upper bound as follows

$$\hat{x}_{\nu 3} \equiv (\hat{x}_\nu)_{33} = \frac{m_{n_3}}{\mu_0} \leq 10^{-3}. \quad (37)$$

To avoid unnecessary independent parameters of  $Y_{Ia}^h$  without any qualitative AMM results discussed on this work, we assume that

$$Y_{Ia}^h = Y_{6a}^h \delta_{I6}, \quad (38)$$

which gives  $(Y^{h\dagger} Y^h)_{aa} = |Y_{6a}^h|^2$ . The total one-loop level contribution arising from the exchange of two singly charged Higgs bosons is written as

$$a_{e_a}(h^\pm) \equiv a_{e_a}(h_1^\pm) + a_{e_a}(h_2^\pm) = a_{e_a,0}(h^\pm) + \dots, \quad (39)$$

$$\begin{aligned} a_{e_a,0}(h^\pm) &= 9.19 \times 10^{-9} f_H \times \frac{m_{e_a}^2}{m_\mu^2} \\ &\times \text{Re} \left\{ \frac{v s_{2\varphi}}{2\sqrt{2}m_{e_a}} U_{\text{PMNS},23} (x_{\nu 3})^{1/2} Y_{6a}^h [x_1 f_\Phi(x_1) - x_2 f_\Phi(x_2)] \right\}, \end{aligned} \quad (40)$$

where  $a_{e_a,0}(h^\pm)$  denotes the dominant term of the chirally-enhanced part coming from the second one in the first line of the real part given in Eq. (35) where  $x_k$  is the part relating with the contribution from  $h_k^\pm$  exchange. This conclusion can be qualitatively understood from the property of the large factor  $v/(2\sqrt{2}m_{e_a})$  as well as large free Yukawa couplings up to the perturbative limit  $|Y_{6a}^h| \leq \sqrt{4\pi}$ . In addition, the sign of this term can be the same as  $\Delta a_{e_a}^{\text{NP}}$  depending on the sign of  $\text{Re}[Y_{6a}^h]$  when all other factors are fixed. As a result, this term can easily explain both signs of  $\Delta a_\mu^{\text{NP}}$  and  $\Delta a_e^{\text{NP}}$  that are still in conflict between different experimental results and needed to be confirmed in the future. Our numerical investigation showed that the term in Eq. (40) is the dominant one, and the sum of all the remaining

terms is suppressed in the allowed regions of parameter space. More detailed estimations confirming that the remaining contributions are suppressed were given in Ref. [94]. Finally,  $a_{e_a,0}(h^\pm) \neq 0$  only when the mixing between two  $SU(2)_L$  doublets and singlets is non-zero  $s_\varphi c_\varphi \neq 0$ , and their masses are non degenerate  $m_{h_1^\pm} \neq m_{h_2^\pm}$ .

Now we consider the case of  $f_H = t_\beta^{-1}$ , which corresponds to the models where the RH neutrino singlets couple with  $\Phi_2$ , whereas the charged leptons couple with  $\Phi_1$  Refs. [57, 94]. Now, increasing values of  $a_{e_a,0}(h^\pm)$  in Eq. (40) require small  $t_\beta$  values, thus implying that the scanning range of  $t_\beta$  should be chosen from the lower bound  $t_\beta \geq 0.4$ . Numerical illustrations of  $a_{e_a,0}(h^\pm)$  are shown in Fig. 1 with fixed  $\hat{x}_{\nu 3} = 10^{-3}$ , i.e.,  $0 \neq |(Y_2^N)_{ab}| < \sqrt{4\pi}$ . In addition,

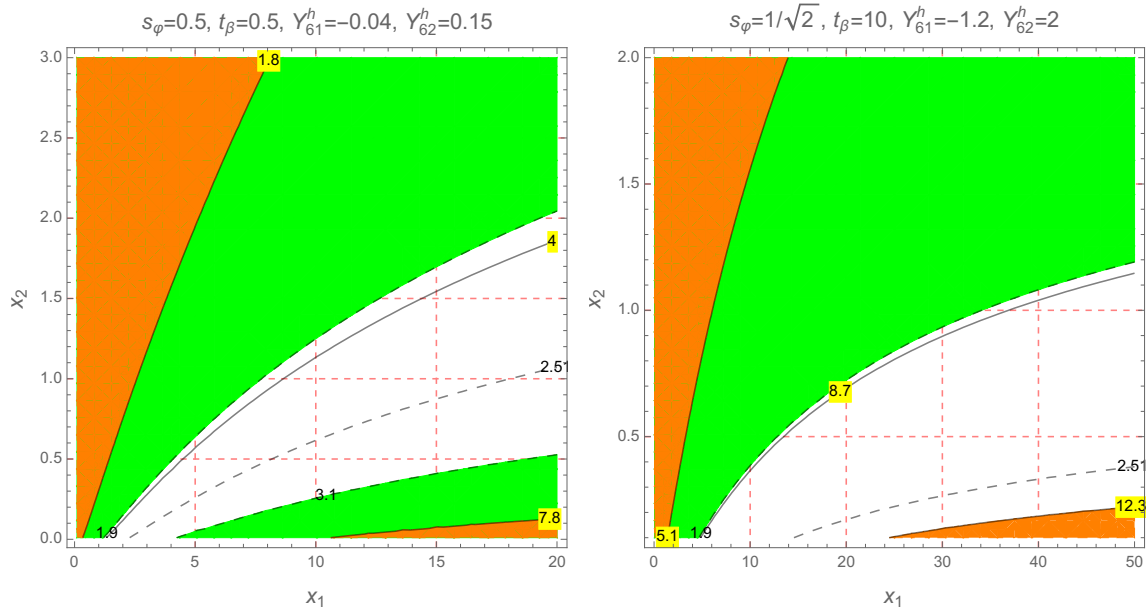


FIG. 1. Contour plots of  $\Delta a_\mu(h^\pm) \times 10^9$  and  $\Delta a_e(h^\pm) \times 10^{13}$  as functions of  $x_1$  and  $x_2$ , where  $\hat{x}_{\nu 3} = 10^{-3}$  and  $f_H = t_\beta^{-1}$ . The green (orange) regions are excluded by the  $1\sigma$  data of  $\Delta a_\mu^{\text{NP}}$  ( $\Delta a_e^{\text{NP}}$ ). The black and dashed-black curves show the constant values of  $\Delta a_e(h^\pm) \times 10^{13}$  and  $\Delta a_\mu(h^\pm) \times 10^9$ , respectively.

there are different fixed values of  $s_\varphi, t_\beta, Y_{61}^h$ , and  $Y_{62}^h$  shown in the respective panels, namely small  $t_\beta = 0.5$  and large  $t_\beta = 10$ . We have checked that  $a_{e_a,0}(h^\pm) \simeq a_{e_a}(h^\pm)$ . Now we estimate the allowed ranges of  $M_0, m_{h_{1,2}^\pm}$ , which are affected from the perturbative limit of the Yukawa coupling matrix  $Y_0^N$  defined in Eq. (25) and related with  $M_0$  through Eqs. (11), (8), and (14). We have two different constraints corresponding to  $f_H = t_\beta^{-1}$  and  $(-t_\beta)$ . The

constraint for  $f_H = t_\beta^{-1}$  is

$$M_0 \left| \left( \hat{x}_\nu^{1/2} U_{\text{PMNS}}^\dagger \right)_{ab} \right| = \frac{vt_\beta}{\sqrt{2}} |c_\beta(Y_2^N)_{(a+3)b}| < \frac{vs_\beta}{\sqrt{2}} \sqrt{4\pi}. \quad (41)$$

We can choose a more strict upper bound of  $M_0 \leq \hat{x}_{\nu 3}^{-1/2} s_\beta v \sqrt{\pi/2} = 9.7 s_\beta$  TeV for  $f_H = t_\beta^{-1}$  and  $\hat{x}_{\nu 3} = 10^{-3}$ . Therefore for  $\hat{x}_{\nu 3} \leq 10^{-3}$  and  $t_\beta \geq 0.4$ , values of  $M_0 \leq 6.4$  TeV are always acceptable. Applying this constraint, we consider a benchmark where  $M_0 = 3$  TeV in order to estimate the allowed values of  $m_{h_1^\pm}$ . We can see that in the left-panel of figure 1, the range  $0.2 \leq x_2 = M_0^2/m_{h_2^\pm}^2 \leq 1.5$  with  $x_1 = M_0^2/m_{h_1^\pm}^2 = 10$  is allowed with respect to  $2.5 \text{ TeV} \leq m_{h_2^\pm} \leq 5 \text{ TeV}$  and  $m_{h_1^\pm} \simeq 0.95 \text{ TeV}$ . Similarly for the right panel of figure 1, we can choose  $M_0 = 5$  TeV and larger  $m_{h_2^\pm} = M_0/\sqrt{0.5}$  and  $m_{h_1^\pm} \geq 5/\sqrt{20} > 1 \text{ TeV}$ .

In the last discussion we will focus on the allowed regions consisting of masses of heavy neutrinos and singly charged Higgs bosons below few TeV so that they can be detected by future colliders. The allowed regions are defined as they result in the two values of  $\Delta a_\mu(h^\pm)$  and  $\Delta a_e(h^\pm)$  both satisfying the experimental data of the muon and electron anomalous magnetic moments within the  $1\sigma$  level, and all perturbative limits of the Yukawa couplings  $Y_{Ia}^h$  and  $Y_{Ia}^X$  are satisfied. The region of parameter space used to scan is chosen as follows:

$$0.8 \text{ TeV} \leq m_{h_1^\pm}, m_{h_2^\pm} \leq 5 \text{ TeV}; 10 \text{ GeV} \leq M_0 \leq 5 \text{ TeV}; \\ 0.3 \leq t_\beta \leq 50; |s_\varphi| \leq 1.; |Y_{Ia}^h|, |Y_{2,Ia}^N| \leq 3; 10^{-7} \leq \hat{x}_{\nu 3} \equiv (\hat{x}_\nu)_{33} = \frac{m_{n_3}}{\mu_X} \leq 10^{-3}. \quad (42)$$

The scanning range of  $\hat{x}_{\nu 3}$  satisfies the non-unitary constraint given in Eq. (19). The numerical results confirm that  $|a_{\mu,0}(h^\pm)/a_\mu(h^\pm)| \simeq 100\%$ , hence the discussion from correlations between different contributions in Eq. (36) will not be shown. The correlations between important free parameters vs.  $a_{\mu,2}(h^\pm)$  are shown in Fig. 2. As mentioned above, large  $t_\beta$  favors small  $\Delta a_\mu(h^\pm)$ , leading to an upper bound on  $t_\beta$  in the allowed regions, see the left-panel of Fig. 2. The correlations of  $\Delta a_\mu(h^\pm)$  and  $\Delta a_e(h^\pm)$  can be seen from the Yukawa couplings  $Y_{61}^h$  in the right panel, where it is bounded in a more strict range than the one given in Eq. (42), see Table I, where other allowed ranges are listed. An interesting property is that excepting  $t_\beta$ , all other parameters like  $M_0$ , the non-unitary parameter  $\hat{x}_{\nu 3}$ ,  $Y_{61,62}^h$ , and  $s_\varphi$  must have lower bounds. The allowed ranges of heavy neutrino masses  $M_0 \geq \mathcal{O}(100)$  GeV might be confirmed by recent experimental searches in colliders such as LHC and ILC [89–93].

The correlations relating the masses with  $\Delta a_\mu(h^\pm)$  are shown in Fig. 3. We can see that

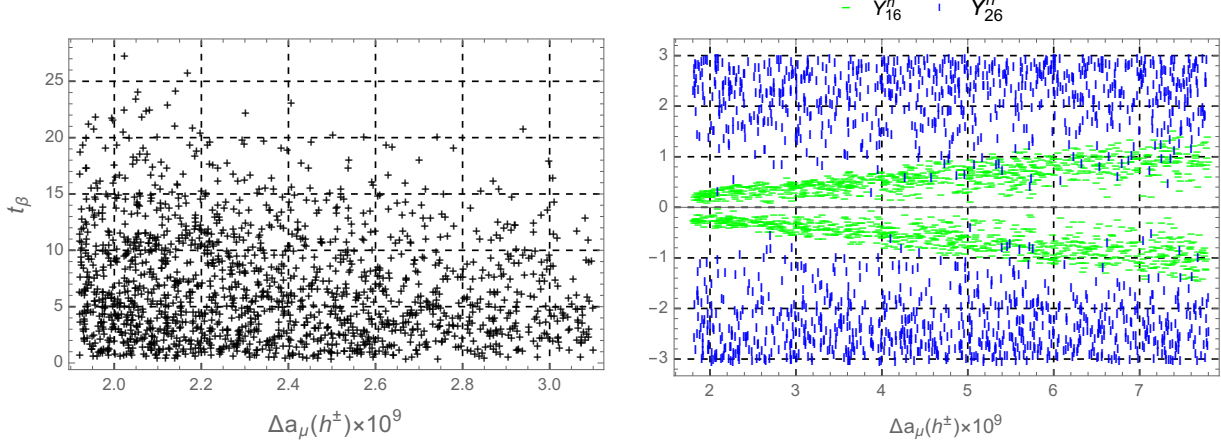


FIG. 2. The correlations of  $\Delta a_\mu(h^\pm)$  vs  $t_\beta$  and  $Y_{61}^h$ ,  $Y_{62}^h$  with  $f_H = t_\beta^{-1}$ .

	$t_\beta$	$ s_\varphi $	$M_0$ [GeV]	$ Y_{61}^h $	$ Y_{62}^h $	$\hat{x}_{\nu 3}$
Min	0.4	0.03	184.6	0.039	0.33	$9.6 \times 10^{-6}$
Max	27.3	0.998	5000	1.506	3	$10^{-3}$

TABLE I. Allowed ranges corresponding to the scanned region given in Eq. (42), considered in case of  $f_H = t_\beta^{-1}$ .

$m_{h_1^\pm}^2$  must be different than  $m_{h_2^\pm}^2$  and our numerical analysis indicates  $|m_{h_2^\pm}^2 - m_{h_1^\pm}^2| \geq 100$  GeV.

Finally, the correlations showing significant dependence of free parameters and  $t_\beta$  are given in Fig. 4, where the allowed regions with large  $t_\beta \geq 20$  require both conditions of large mixing  $|s_{2\varphi}| = 1$  and large  $\hat{x}_{\nu 3}$ . We obtain a small allowed range of  $t_\beta \leq 10$  that was missed in Ref. [54]. Our result is consistent with the discussion corresponding to 3-3-1 models given in Ref. [95], where the THDM is embedded.

For the case of  $f_H = (-t_\beta)$ , i.e., RH neutrino and charged leptons singlets couple with the same  $SU(2)_L$  Higgs doublet  $\Phi_1$  in Yukawa Lagrangian (6), for example Ref. [95]. Then large  $a_{e_a}(h^\pm)$  in Eq. (40) support large  $t_\beta$ . In addition, even when  $a_{e_a}(h^\pm) \sim s_{2\varphi} \neq 0$ , the first terms in the first lines of Eq. (35) or (36) may be large enough consistent with  $\Delta a_{\mu,e}^{\text{NP}}$  in both sign and amplitude. But the simple assumptions of the couplings and the total neutrino mass matrix in this work are not enough to explain both  $(g-2)_{e,\mu}$  experimental

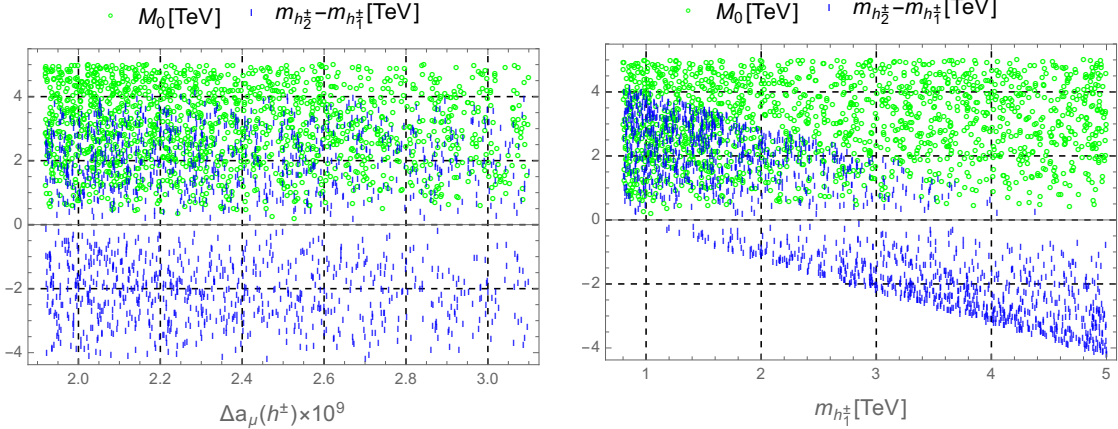


FIG. 3. The correlations of  $\Delta a_\mu(h^\pm)$  and  $m_{h_1^\pm}$  vs. masses  $M_0$ ,  $m_{h_{1,2}^\pm}$ , with  $f_H = t_\beta^{-1}$ .

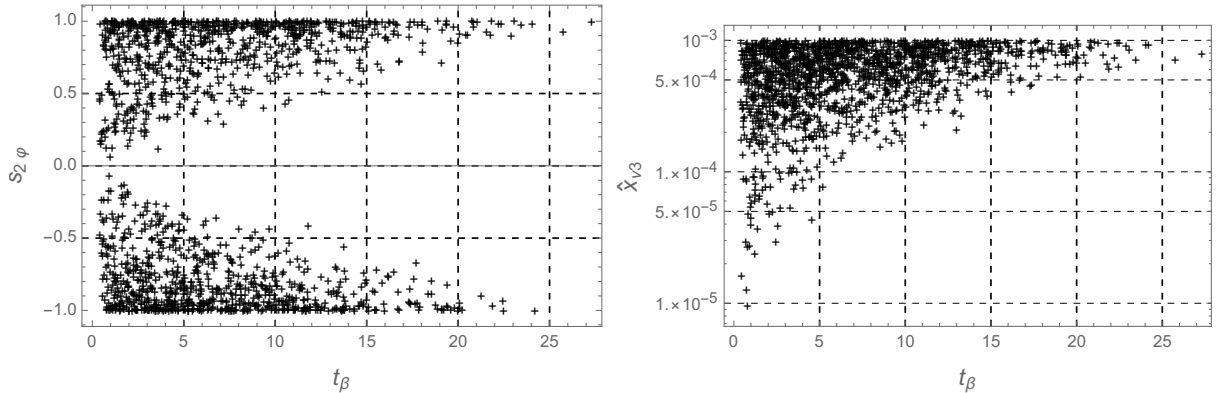


FIG. 4. The correlations of  $t_\beta$  vs other free parameters in the allowed regions with  $f_H = t_\beta^{-1}$ .

data. The perturbative constraint gives an upper bound on  $M_0$ , namely

$$M_0 \left| \left( \hat{x}_\nu^{1/2} U_{\text{PMNS}}^\dagger \right)_{ab} \right| = \frac{v c_\beta}{\sqrt{2}} |(Y_1^N)_{(a+3)b}| \Rightarrow M_0 < \hat{x}_{\nu,3}^{-1/2} |U_{\text{PMNS},23}|^{-1} v c_\beta \sqrt{2\pi}, \quad (43)$$

therefore  $M_0$  may be small with small  $c_\beta$  equivalently with large  $t_\beta$ . We always have  $M_0 < 1.6$  TeV for  $t_\beta = 0.4$  and  $\hat{x}_{\nu,3} = 10^{-3}$ . Although  $t_\beta \geq 0.4$  is always kept, smaller  $\hat{x}_{\nu,3} \leq 10^{-3}$  may allow large  $M_0$  which also allow large  $m_{h_{1,2}^\pm}$ . On the other hand, from Eq. (40),  $|a_{e_a}| \sim t_\beta (x_{\nu 3})^{1/2} |s_{2\varphi} Y_{6a}^h|$ , hence the allowed regions are easily satisfied for small  $t_\beta$  and large values of other parameters. Our numerical analysis shows that large  $x_{\nu 3} \geq 10^{-4}$  allows all  $t_\beta \leq 50$  and all singly charged Higgs masses at the TeV scale. Contour plots of  $\Delta a_\mu(h^\pm) \times 10^9$  and  $\Delta a_e(h^\pm) \times 10^{13}$  for  $\hat{x}_{\nu,3} = 5 \times 10^{-4}$  with small  $t_\beta = 0.5$  and large  $t_\beta = 20$  are shown in Fig. 5.

Regarding the numerical analysis in the scanning range (42) with  $f_H = -t_\beta$ , the allowed

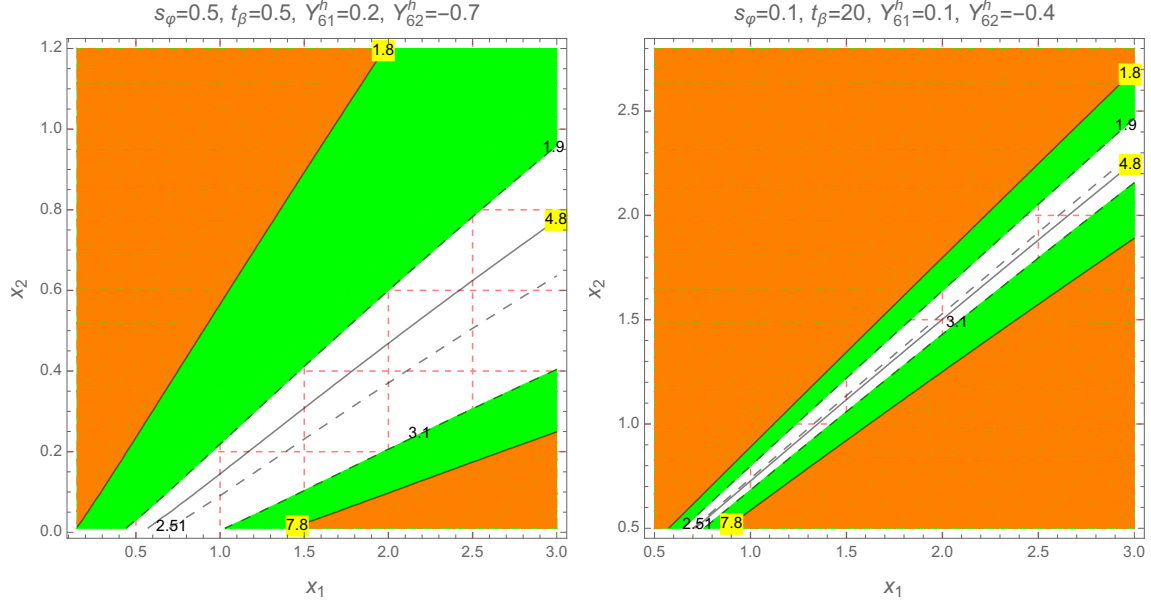


FIG. 5. Contour plots of  $\Delta a_\mu(h^\pm) \times 10^9$  and  $\Delta a_e(h^\pm) \times 10^{13}$  as functions of  $x_1$  and  $x_2$ , where  $\hat{x}_{\nu 3} = 5 \times 10^{-4}$  and  $f_H = -t_\beta$ . The green (orange) regions are excluded by the  $1\sigma$  data of  $\Delta a_\mu^{\text{NP}}$  ( $\Delta a_e^{\text{NP}}$ ). The black and dashed-black curves show the constant values of  $\Delta a_e(h^\pm) \times 10^{13}$  and  $\Delta a_\mu(h^\pm) \times 10^9$ , respectively.

ranges are tighter than the scanning regions as shown below

$$|s_\varphi| \geq 0.003, 1.585 \geq |Y_{61}^h| \geq 0.008, |Y_{62}^h| \geq 0.034, \hat{x}_{\nu 3} \geq 10^{-7}. \quad (44)$$

The numerical results of the correlations between  $t_\beta$  vs.  $Y_{61}^h$ ,  $Y_{62}^h$ , and  $\hat{x}_{\nu 3}$  are shown in Fig. 6, where the allowed ranges of  $Y_{62}^h$  correspond to a rather narrow allowed range of  $Y_{61}^h$ , see Eq. (44). This implies that the phenomenology of the singly charged Higgs boson at colliders related with these two couplings will have some certain relations that should be experimentally verified.

Finally, we have comments regarding the  $(g-2)_e$  data [26]:  $\Delta a_e^{\text{NP}} = -(8.7 \pm 3.6) \times 10^{-13}$ . The allowed regions of parameter space corresponding to this data can be derived from the above described numerical analysis. Namely, excepting  $Y_{61}^h$  all allowed ranges of free parameters are kept unchanged to guarantee consistency with the experimental  $(g-2)_\mu$  data. On the other hand,  $Y_{61}^h$  is changed into new values that  $Y_{61}^h \rightarrow \frac{(-8.7 \pm 3.6)}{(4.8 \pm 3)} \times Y_{61}^h$  and exclude too large values violating the perturbative limit.

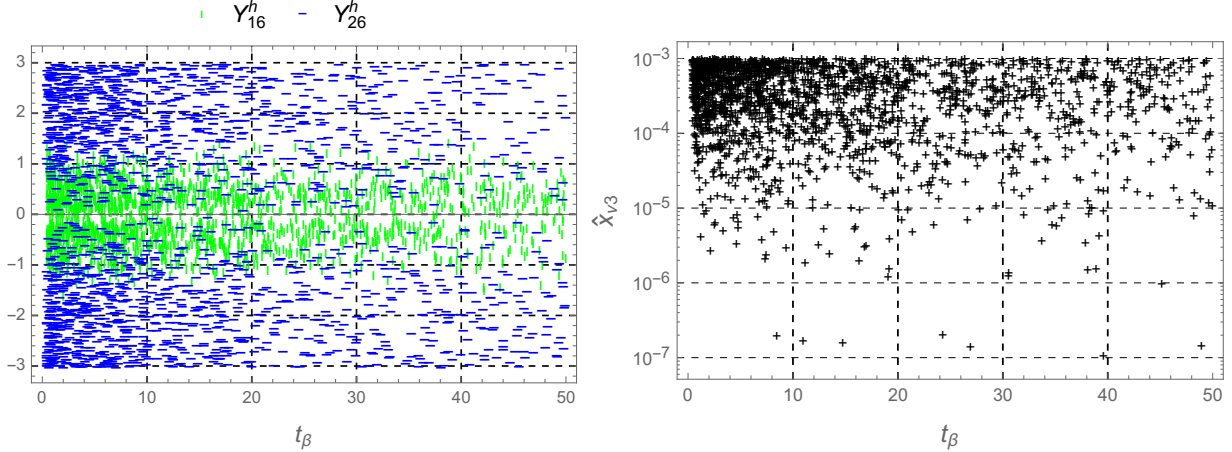


FIG. 6. The correlations of  $t_\beta$  vs other free parameters in the allowed regions with  $f_H = -t_\beta$ .

#### IV. CONCLUSION

In this work we have shown that the appearance of heavy ISS neutrinos and singly charged Higgs bosons is a very promising solution to explain the experimental data on both  $(g - 2)_{\mu,e}$  anomalies in many different types of THDM, and in regions of parameter space allowing heavy singly charged Higgs boson masses up to the TeV scale and small values of the  $\tan \beta$  parameter satisfying  $\tan \beta \geq 0.4$ . Hence, this solution will enlarge the allowed regions of parameter spaces of the THDM which can simultaneously explain the  $(g - 2)_{e,\mu}$  data thanks to the one loop exchange of electrically charged Higgs bosons with masses within the LHC reach.

#### ACKNOWLEDGMENTS

This research is funded by the Vietnam National Foundation for Science and Technology Development (NAFOSTED) under the grant number 103.01-2019.387 as well as by ANID-Chile FONDECYT 1210378, ANID PIA/APOYO AFB180002 and Milenio-ANID-ICN2019\_044.

---

[1] B. Abi *et al.* [Muon g-2], Phys. Rev. Lett. **126**, 141801 (2021) [arXiv:2104.03281 [hep-ex]].

- [2] G. W. Bennett *et al.* [Muon g-2], Phys. Rev. D **73**, 072003 (2006) [arXiv:hep-ex/0602035 [hep-ex]].
- [3] T. Aoyama, N. Asmussen, M. Benayoun, J. Bijnens, T. Blum, M. Bruno, I. Caprini, C. M. Carloni Calame, M. Cè and G. Colangelo, *et al.* Phys. Rept. **887**, 1 (2020) [arXiv:2006.04822 [hep-ph]].
- [4] A. Keshavarzi, D. Nomura and T. Teubner, Phys. Rev. D **97**, no.11, 114025 (2018) [arXiv:1802.02995 [hep-ph]].
- [5] G. Colangelo, M. Hoferichter and P. Stoffer, JHEP **02**, 006 (2019) [arXiv:1810.00007 [hep-ph]].
- [6] M. Hoferichter, B. L. Hoid and B. Kubis, JHEP **08**, 137 (2019) [arXiv:1907.01556 [hep-ph]].
- [7] M. Davier, A. Hoecker, B. Malaescu and Z. Zhang, Eur. Phys. J. C **80**, no.3, 241 (2020) [erratum: Eur. Phys. J. C **80**, no.5, 410 (2020)] [arXiv:1908.00921 [hep-ph]].
- [8] A. Keshavarzi, D. Nomura and T. Teubner, Phys. Rev. D **101**, no.1, 014029 (2020) [arXiv:1911.00367 [hep-ph]].
- [9] A. Kurz, T. Liu, P. Marquard and M. Steinhauser, Phys. Lett. B **734**, 144-147 (2014) [arXiv:1403.6400 [hep-ph]].
- [10] K. Melnikov and A. Vainshtein, Phys. Rev. D **70**, 113006 (2004) [arXiv:hep-ph/0312226 [hep-ph]].
- [11] P. Masjuan and P. Sanchez-Puertas, Phys. Rev. D **95**, no.5, 054026 (2017) [arXiv:1701.05829 [hep-ph]].
- [12] G. Colangelo, M. Hoferichter, M. Procura and P. Stoffer, JHEP **04**, 161 (2017) [arXiv:1702.07347 [hep-ph]].
- [13] M. Hoferichter, B. L. Hoid, B. Kubis, S. Leupold and S. P. Schneider, JHEP **10**, 141 (2018) [arXiv:1808.04823 [hep-ph]].
- [14] A. Gérardin, H. B. Meyer and A. Nyffeler, Phys. Rev. D **100**, no.3, 034520 (2019) [arXiv:1903.09471 [hep-lat]].
- [15] J. Bijnens, N. Hermansson-Truedsson and A. Rodríguez-Sánchez, Phys. Lett. B **798**, 134994 (2019) [arXiv:1908.03331 [hep-ph]].
- [16] G. Colangelo, F. Hagelstein, M. Hoferichter, L. Laub and P. Stoffer, JHEP **03**, 101 (2020) [arXiv:1910.13432 [hep-ph]].
- [17] G. Colangelo, M. Hoferichter, A. Nyffeler, M. Passera and P. Stoffer, Phys. Lett. B **735**, 90-91 (2014) [arXiv:1403.7512 [hep-ph]].

[18] T. Blum, N. Christ, M. Hayakawa, T. Izubuchi, L. Jin, C. Jung and C. Lehner, Phys. Rev. Lett. **124**, no.13, 132002 (2020) [arXiv:1911.08123 [hep-lat]].

[19] T. Aoyama, M. Hayakawa, T. Kinoshita and M. Nio, Phys. Rev. Lett. **109**, 111808 (2012) [arXiv:1205.5370 [hep-ph]].

[20] T. Aoyama, T. Kinoshita and M. Nio, Atoms **7**, no.1, 28 (2019)

[21] A. Czarnecki, W. J. Marciano and A. Vainshtein, Phys. Rev. D **67**, 073006 (2003) [erratum: Phys. Rev. D **73**, 119901 (2006)] [arXiv:hep-ph/0212229 [hep-ph]].

[22] C. Gnendiger, D. Stöckinger and H. Stöckinger-Kim, Phys. Rev. D **88**, 053005 (2013) [arXiv:1306.5546 [hep-ph]].

[23] M. Davier, A. Hoecker, B. Malaescu and Z. Zhang, Eur. Phys. J. C **77**, no.12, 827 (2017) [arXiv:1706.09436 [hep-ph]].

[24] M. Davier, A. Hoecker, B. Malaescu and Z. Zhang, Eur. Phys. J. C **71**, 1515 (2011) [erratum: Eur. Phys. J. C **72**, 1874 (2012)] [arXiv:1010.4180 [hep-ph]].

[25] D. Hanneke, S. Fogwell and G. Gabrielse, Phys. Rev. Lett. **100**, 120801 (2008) [arXiv:0801.1134 [physics.atom-ph]].

[26] R. H. Parker, C. Yu, W. Zhong, B. Estey and H. Müller, Science **360**, 191 (2018) [arXiv:1812.04130 [physics.atom-ph]].

[27] L. Morel, Z. Yao, P. Cladé and S. Guellati-Khélifa, Nature **588**, no.7836, 61-65 (2020)

[28] T. Aoyama, M. Hayakawa, T. Kinoshita and M. Nio, Phys. Rev. Lett. **109**, 111807 (2012) [arXiv:1205.5368 [hep-ph]].

[29] S. Laporta, Phys. Lett. B **772**, 232-238 (2017) [arXiv:1704.06996 [hep-ph]].

[30] T. Aoyama, T. Kinoshita and M. Nio, Phys. Rev. D **97**, no.3, 036001 (2018) [arXiv:1712.06060 [hep-ph]].

[31] H. Terazawa, Nonlin. Phenom. Complex Syst. **21**, no.3, 268-272 (2018)

[32] S. Volkov, Phys. Rev. D **100**, no.9, 096004 (2019) [arXiv:1909.08015 [hep-ph]].

[33] A. Gérardin, Eur. Phys. J. A **57**, no.4, 116 (2021) [arXiv:2012.03931 [hep-lat]].

[34] R. Dermisek and A. Raval, Phys. Rev. D **88**, 013017 (2013) [arXiv:1305.3522 [hep-ph]].

[35] A. Crivellin, M. Hoferichter and P. Schmidt-Wellenburg, Phys. Rev. D **98**, no.11, 113002 (2018) [arXiv:1807.11484 [hep-ph]].

[36] P. Escribano, J. Terol-Calvo and A. Vicente, Phys. Rev. D **103**, no.11, 115018 (2021) [arXiv:2104.03705 [hep-ph]].

- [37] A. Crivellin and M. Hoferichter, JHEP **07**, 135 (2021) [arXiv:2104.03202 [hep-ph]].
- [38] R. Dermisek, K. Hermanek and N. McGinnis, [arXiv:2103.05645 [hep-ph]].
- [39] A. E. C. Hernández, S. F. King and H. Lee, Phys. Rev. D **103**, no.11, 115024 (2021) [arXiv:2101.05819 [hep-ph]].
- [40] E. J. Chun and T. Mondal, JHEP **11**, 077 (2020) [arXiv:2009.08314 [hep-ph]].
- [41] M. Frank and I. Saha, Phys. Rev. D **102**, no.11, 115034 (2020) [arXiv:2008.11909 [hep-ph]].
- [42] K. F. Chen, C. W. Chiang and K. Yagyu, JHEP **09**, 119 (2020) [arXiv:2006.07929 [hep-ph]].
- [43] P. M. Ferreira, B. L. Gonçalves, F. R. Joaquim and M. Sher, Phys. Rev. D **104**, no.5, 053008 (2021) [arXiv:2104.03367 [hep-ph]].
- [44] M. Endo and S. Mishima, JHEP **08**, no.08, 004 (2020) [arXiv:2005.03933 [hep-ph]].
- [45] C. Hati, J. Kriewald, J. Orloff and A. M. Teixeira, JHEP **07**, 235 (2020) [arXiv:2005.00028 [hep-ph]].
- [46] D. Borah, M. Dutta, S. Mahapatra and N. Sahu, [arXiv:2109.02699 [hep-ph]].
- [47] H. Bharadwaj, S. Dutta and A. Goyal, [arXiv:2109.02586 [hep-ph]].
- [48] A. S. De Jesus, S. Kovalenko, F. S. Queiroz, C. Siqueira and K. Sinha, Phys. Rev. D **102**, no.3, 035004 (2020) [arXiv:2004.01200 [hep-ph]].
- [49] D. Cogollo, Y. M. Oviedo-Torres and Y. S. Villamizar, Int. J. Mod. Phys. A **35**, no.23, 2050126 (2020) [arXiv:2004.14792 [hep-ph]].
- [50] B. D. Sáez and K. Ghorbani, [arXiv:2107.08945 [hep-ph]].
- [51] A. Crivellin, D. Mueller and F. Saturnino, Phys. Rev. Lett. **127**, no.2, 021801 (2021) [arXiv:2008.02643 [hep-ph]].
- [52] D. Zhang, JHEP **07**, 069 (2021) [arXiv:2105.08670 [hep-ph]].
- [53] W. Y. Keung, D. Marfatia and P. Y. Tseng, LHEP **2021**, 209 (2021) [arXiv:2104.03341 [hep-ph]].
- [54] T. Mondal and H. Okada, [arXiv:2103.13149 [hep-ph]].
- [55] D. W. Kang, J. Kim and H. Okada, Phys. Lett. B **822**, 136666 (2021) [arXiv:2107.09960 [hep-ph]].
- [56] A. E. Cárcamo Hernández, C. Espinoza, J. Carlos Gómez-Izquierdo and M. Mondragón, [arXiv:2104.02730 [hep-ph]].
- [57] S. P. Li, X. Q. Li, Y. Y. Li, Y. D. Yang and X. Zhang, JHEP **01**, 034 (2021) [arXiv:2010.02799 [hep-ph]].

[58] L. Delle Rose, S. Khalil and S. Moretti, Phys. Lett. B **816**, 136216 (2021) [arXiv:2012.06911 [hep-ph]].

[59] F. J. Botella, F. Cornet-Gomez and M. Nebot, Phys. Rev. D **102**, no.3, 035023 (2020) [arXiv:2006.01934 [hep-ph]].

[60] X. F. Han, T. Li, H. X. Wang, L. Wang and Y. Zhang, [arXiv:2104.03227 [hep-ph]].

[61] C. H. Chen, C. W. Chiang and T. Nomura, Phys. Rev. D **104**, no.5, 055011 (2021) [arXiv:2104.03275 [hep-ph]].

[62] M. Aoki, S. Kanemura, K. Tsumura and K. Yagyu, Phys. Rev. D **80**, 015017 (2009) [arXiv:0902.4665 [hep-ph]].

[63] A. Jueid, J. Kim, S. Lee and J. Song, [arXiv:2104.10175 [hep-ph]].

[64] P. Athron, C. Balázs, D. H. Jacob, W. Kotlarski, D. Stöckinger and H. Stöckinger-Kim, [arXiv:2104.03691 [hep-ph]].

[65] M. Badziak and K. Sakurai, JHEP **10** (2019), 024 [arXiv:1908.03607 [hep-ph]].

[66] S. Li, Y. Xiao and J. M. Yang, [arXiv:2107.04962 [hep-ph]].

[67] B. Dutta, S. Ghosh and T. Li, Phys. Rev. D **102**, no.5, 055017 (2020) [arXiv:2006.01319 [hep-ph]].

[68] A. E. Cárcamo Hernández, S. Kovalenko, R. Pasechnik and I. Schmidt, JHEP **06**, 056 (2019) [arXiv:1901.02764 [hep-ph]].

[69] A. E. C. Hernández, D. T. Huong and I. Schmidt, [arXiv:2109.12118 [hep-ph]].

[70] A. E. Cárcamo Hernández, S. Kovalenko, R. Pasechnik and I. Schmidt, Eur. Phys. J. C **79**, no.7, 610 (2019) [arXiv:1901.09552 [hep-ph]].

[71] R. Adhikari, I. A. Bhat, D. Borah, E. Ma and D. Nanda, [arXiv:2109.05417 [hep-ph]].

[72] J. Herrero-García, T. Ohlsson, S. Riad and J. Wirén, JHEP **04**, 130 (2017) [arXiv:1701.05345 [hep-ph]].

[73] S. Davidson and H. E. Haber, Phys. Rev. D **72**, 035004 (2005) [erratum: Phys. Rev. D **72**, 099902 (2005)] [arXiv:hep-ph/0504050 [hep-ph]].

[74] L. Allwicher, P. Arnan, D. Barducci and M. Nardecchia, [arXiv:2108.00013 [hep-ph]].

[75] P. A. Zyla *et al.* [Particle Data Group], PTEP **2020**, 083C01 (2020)

[76] A. Ibarra, E. Molinaro and S. T. Petcov, JHEP **09**, 108 (2010) [arXiv:1007.2378 [hep-ph]].

[77] E. Arganda, M. J. Herrero, X. Marcano and C. Weiland, Phys. Rev. D **91**, 015001 (2015) [arXiv:1405.4300 [hep-ph]].

[78] J. A. Casas and A. Ibarra, Nucl. Phys. B **618**, 171 (2001) [arXiv:hep-ph/0103065 [hep-ph]].

[79] A. M. Baldini *et al.* [MEG], Eur. Phys. J. C **76**, no.8, 434 (2016) [arXiv:1605.05081 [hep-ex]].

[80] B. Aubert *et al.* [BaBar], Phys. Rev. Lett. **104**, 021802 (2010) [arXiv:0908.2381 [hep-ex]].

[81] N. Aghanim *et al.* [Planck], Astron. Astrophys. **641**, A6 (2020) [erratum: Astron. Astrophys. **652**, C4 (2021)] [arXiv:1807.06209 [astro-ph.CO]]

[82] J. P. Pinheiro, C. A. d. S. Pires, F. S. Queiroz and Y. S. Villamizar, [arXiv:2107.01315 [hep-ph]].

[83] E. Fernandez-Martinez, J. Hernandez-Garcia and J. Lopez-Pavon, JHEP **08**, 033 (2016) [arXiv:1605.08774 [hep-ph]].

[84] N. R. Agostinho, G. C. Branco, P. M. F. Pereira, M. N. Rebelo and J. I. Silva-Marcos, Eur. Phys. J. C **78**, no.11, 895 (2018) [arXiv:1711.06229 [hep-ph]].

[85] T. N. Dao, M. Mühlleitner and A. V. Phan, [arXiv:2108.10088 [hep-ph]].

[86] C. Biggio, E. Fernandez-Martinez, M. Filaci, J. Hernandez-Garcia and J. Lopez-Pavon, JHEP **05**, 022 (2020) [arXiv:1911.11790 [hep-ph]].

[87] F. Jegerlehner and A. Nyffeler, Phys. Rept. **477**, 1-110 (2009) [arXiv:0902.3360 [hep-ph]].

[88] A. Nepomuceno and B. Meirose, Phys. Rev. D **101**, 035017 (2020) [arXiv:1911.12783 [hep-ph]].

[89] A. Das and N. Okada, Phys. Rev. D **88**, 113001 (2013) [arXiv:1207.3734 [hep-ph]].

[90] A. Das, P. S. Bhupal Dev and N. Okada, Phys. Lett. B **735**, 364-370 (2014) [arXiv:1405.0177 [hep-ph]].

[91] A. Das and N. Okada, Phys. Rev. D **93**, no.3, 033003 (2016) [arXiv:1510.04790 [hep-ph]].

[92] A. Das, P. Konar and S. Majhi, JHEP **06**, 019 (2016) [arXiv:1604.00608 [hep-ph]].

[93] A. Das, S. Jana, S. Mandal and S. Nandi, Phys. Rev. D **99**, no.5, 055030 (2019) [arXiv:1811.04291 [hep-ph]].

[94] L. T. Hue, K. H. Phan, T. P. Nguyen, H. N. Long and H. T. Hung, [arXiv:2109.06089 [hep-ph]].

[95] L. T. Hue, H. T. Hung, N. T. Tham, H. N. Long and T. P. Nguyen, Phys. Rev. D **104**, 033007 (2021) [arXiv:2104.01840 [hep-ph]].